Thin–Walled Structures 157 (2020) 106984

Contents lists available at ScienceDirect

Thin-Walled Structures

journal homepage: http://www.elsevier.com/locate/tws

Full length article

Preload loss of stainless steel bolts in aluminium plated slip resistant connections

Christiaan den Otter [a], Johan Maljaars [a,b,*]

[a] Eindhoven University of Technology, Department of the Built Environment, Delft, the Netherlands
[b] TNO, Department of Structural Reliability, Delft, the Netherlands

ARTICLE INFO

Keywords:
Creep
Relaxation
Viscoplasticity
Bolt
Lateral contraction
Stainless steel
Aluminium slip resistant connection
Reliability analysis
Partial factor

ABSTRACT

Bolted connections are applied in many aluminium structures. Stainless steel bolts are often preferred over carbon steel bolts in aluminium connections to prevent galvanic corrosion. However, current design standards and guidelines do not allow for using preloaded stainless steel bolts in slip resistant connections, mainly because of a lack of knowledge on the preload loss to be expected in these connections, and this limits the application field of this type of structure. This paper presents a combined empirical and analytical (i.e. mechanical) study into preload losses of stainless steel bolts in aluminium slip resistant connections caused by long-term effects (creep and relaxation), thermal expansion, and lateral contraction. It appears that stainless steel bolts can be applied in aluminium slip resistant connections, but a larger partial safety factor than standards currently prescribe is required for the slip resistance in ultimate limit state.

1. Introduction

Bolted connections allow for creating simple, demountable, and adjustable connections in a short construction time without the need of very special equipment. Bolted connections can be highly cost effective under specific circumstances and they are therefore widely applied in civil, building, and marine applications. Bolts can be applied in tension and in shear connections. This study concerns the latter type of connection. It may be advantageous to preload the bolts with a controlled tightening procedure in combination with a certain surface treatment of the plates in order to obtain a certain minimum friction coefficient. Shear forces applied to the connection are then (primarily) transferred through friction between plates, washers, bolt head and nut, instead of through bearing. The connection is then referred to as a slip resistant connection. This has the following advantages: 1) Loosening of nuts is prevented so that a locking mechanism is not required; 2) Relative motion of the bolted plates is prevented, resulting into a higher connection stiffness that does not produce noise when reversely loaded; 3) The fatigue life is enhanced; 4) The risk of crevice corrosion is reduced.

Various controlled tightening procedures exist, including an applied controlled torque (torque method), an applied torque followed by a specified part turn or deformation (combined method), a shear wrench on bolts with break-neck (HRC method) and tightening using compressible washers (direct tension indicator method). Variations in the friction coefficient between bolt head or nut and torque wrench, thread variations and tolerances, and variations in the surface condition under the nut cause that the preload force introduced is subject to uncertainty, especially when using the torque method, resulting in a 10% [1] or even 30% [2] variation of the mean preload level in case of lubricated bolts. The European standard EN 1090-2 [3] specifies a nominal minimum preload force, $F_{cl,nom}$, equal to 70% of the tensile strength of the bolt:

$$F_{cl,nom} = 0.7 f_{ub,nom} A_s \quad (1)$$

where:

$f_{ub,nom}$ = nominal ultimate strength of the bolt material
A_s = tensile stress area of the bolt.

The origin of the factor 0.7 is that the 0.2% proof stress in the threaded shaft of the bolt is, depending on the material, equal to or larger than 70% of the tensile strength [4,5], hence the equation preserves a minimum stress equal to the proof strength in the threaded shaft. This nominal preload force corresponds to the 80% fraction of the

Abbreviations: SLS, serviceability limit state; ULS, ultimate limit state; FORM, first order reliability method; V, coefficient of variation.

* Corresponding authorTNO, Department of Structural Reliability, Delft, the Netherlands,
E-mail address: j.maljaars@tue.nl (J. Maljaars).

https://doi.org/10.1016/j.tws.2020.106984
Received 27 February 2020; Received in revised form 20 May 2020; Accepted 15 July 2020
Available online 23 August 2020

Nomenclature

A = area
A_s = tensile stress area
A_d = nominal cross section unthreaded part
A_{d_3} = cross section of thread at minor diamete
C = uncertainty factor for creep strain
D_{1a} = maximum minor diameter nut
E = Young's modulus
$\Delta F_{cl,\dot{\varepsilon}}$ = preload loss due to viscoplastic material behaviour
$\Delta F_{cl,\theta}$ = preload loss due to thermal action
$\Delta F_{cl,\nu}$ = preload loss due to lateral contraction
F_a = applied load
F_{cl} = preload
F_{slip} = slip force
$M_{(x)}$ = mean of variable $\hat{x}$
P = probability
P_f = failure probability
R_a = mean surface roughness
S = deviatoric stress
$S_{(x)}$ = standard deviation of variable $\hat{x}$
T = plate thickness
T_w = washer thickness
d = bolt diameter
d_0 = bolt hole diameter
d_3 = minor diameter of the bolt thread
d_a = minimum major diameter bolt
d_s = diameter of the tensile area of the bolt
d_{wi} = inner diameter of washer
d_W = bearing surface outside diameter
$f_{0.2}$ = 0.2% proof stress
f_j = force fraction transferred through pitch j
f_u = tensile strength
$f(\sigma)$ = stress dependency function
g = limit state function
$k_{(x)}$ = spring stiffness of assembly part x
l = length
l_{SK} = substitutional extension length for the deformation of the bolt head
l_d = length of the unthreaded part
l_g = grip length
l_t = length of the threaded part located in the grip
l_G = substitutional extension length for the deformation of the engaged thread
l_M = substitutional extension length for the deformation of the nut
m = number of contact planes
n = Ramberg Osgood exponent
p = pitch height
t = time
t_e = intended life
u = deformation
w = width of the plates
z = height
α = coefficient of linear thermal expansion
α_R = FORM sensitivity factor for the resistance
β = reliability index
β_{tar} = required reliability index
γ = partial safety factor
ε = strain
$\varepsilon_{cr,em}$ = embedment creep strain
ε_{el} = elastic strain
Φ = cumulative distribution function of the standard normal distribution
ϕ_D = angle of the substitutional deformation cone
θ = temperature
μ = friction coefficient
ν = Poisson ratio
σ = stress
σ_{VM} = Von Mises stress
χ = ratio between the clamping force and the tensile strength

Subscripts

$_0$ = at time $t = 0$ (i.e. directly after tightening or without an external load applies)
$_a$ = applied
$_b$ = bolt assembly, including bolt and nut
$_c$ = characteristic value
$_{cr}$ = creep or relaxation
$_d$ = design value
$_i$ = connection assembly part
$_{nom}$ = nominal value
$_p$ = plate assembly, including plates and washers
$_t$ = at time t

preload force distribution when using the torque or HRC method, or the 95% or higher fraction when using one of the other methods [6].

Bolted connections are often applied in aluminium structures, as these do not have the disadvantage of a local strength reduction that occurs in case of welding, in the heat affected zone. Stainless steel bolts are preferred in connections with aluminium plates when applied in a non-controlled or aggressive environment, in order to prevent galvanic corrosion. However, standards and guidelines do not allow for a stainless steel preloaded bolt to be applied in a slip resistant connection, unless the performance is proven by tests for a specific application [7]. Reasons are a lack of knowledge on the preload loss over time due to viscoplastic deformation of the stainless steel bolt material, a lack of controlled tightening procedures for stainless steel bolts, and the potential risk of galling [8]. These risks are, however, mitigated by recent work of Stranghöner et al.: A tightening procedure was established using suited lubricants [9] and galling can be avoided [9]. Preload loss in stainless steel bolted assemblies was measured and appeared similar to that of carbon steel [8]. And friction coefficients for grit blasted surfaces were $0.4 \leq \mu \leq 0.5$ [10] and therefore in agreement with those for carbon steel, [3]. The issue of corrosion in aluminium connections limits the number of suited lubricants, but there are suited lubricants for which widespread practical experience is available.

The research conducted in Ref. [7–9] concerned various types of stainless steel bolts with stainless steel or carbon steel plates. The behaviour of the plate assembly may, however, be different if aluminium plates are used. Creep and stress relaxation in the steel plates appeared negligible in Ref. [8], but aluminium alloys are generally more sensitive to viscoplastic behaviour. In addition, the material is softer, the modulus of elasticity is lower, and the coefficient of thermal expansion is higher as compared to steel. These aspects may influence the performance of the connections. This paper presents the results of an empirical study into the time dependent effects (embedment creep, bolt relaxation, aluminium creep) and effects caused by external actions (thermal action, lateral contraction due to an applied force) that may affect the preload in carbon or stainless steel bolts in aluminium plated slip resistant connections. Using Eq. (1) implies that the stainless steel grade applied for the bolts should have an 0.2% proof stress that is at least 70% of the tensile strength. Austenitic stainless steel grade 316 – A4 80, also

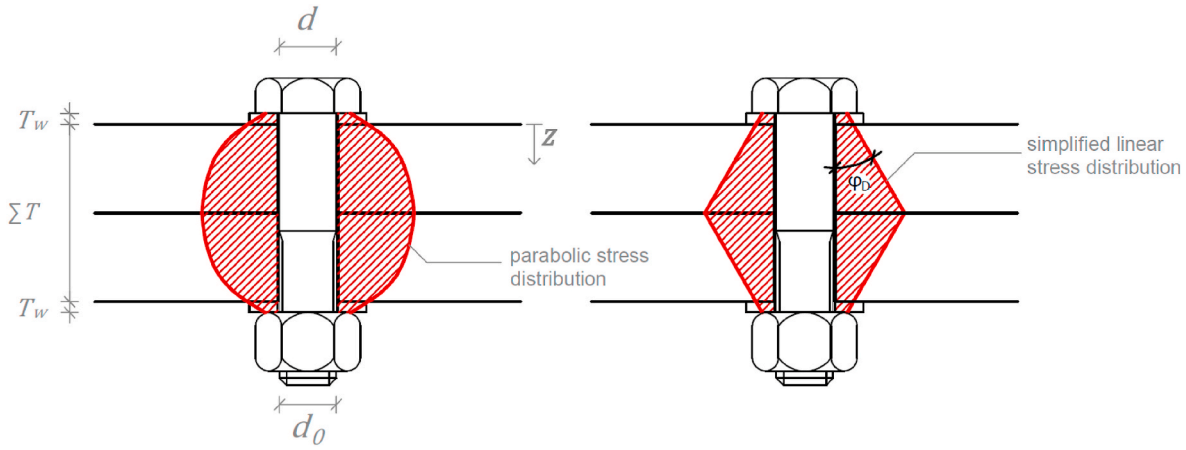

Fig. 1. Realistic parabolic stress distribution in a preloaded bolted connection (left) and simplified linear stress distribution following VDI 2230 [11] (right).

known as EN 1.4401, satisfies this condition and the tests were performed with bolts of this grade. Aluminium alloy AA 5083-H111 is a relatively soft alloy widely applied in structural applications and this alloy was used for the plates.

A theoretical model based on applied mechanics is subsequently used for a parameter study including various geometries and a stronger alloy, namely AA 6061-T6, in addition to the alloy used in the test. The model consists of (linear elastic) springs that represent the various parts constituting the connection. Because of equilibrium of force and deformation in the connection, the loss of preload, $\Delta F_{cl} = F_{cl,t} - F_{cl,0}$, is as follows linked to a certain applied deformation, $\Delta u = u_t - u_0$:

$$\Delta F_{cl} = \Delta u \frac{k_b k_p}{k_b + k_p} \tag{2}$$

where k_b is the stiffness of bolt and nut and k_p is the stiffness of the plates and washers. The stiffness values are determined with the spring model of VDI 2230 [11], see the appendix of this paper.

VDI 2230 [11] assumes a conical frustum to describe the stress in the plate assembly, as presented in Fig. 1 (right) to establish the spring stiffness. This is a simplification of the parabolic stress distribution that is considered more realistic, Fig. 1 (left). The angle of the substitutional deformation cone ϕ_D is selected in such a way, that the stiffness corresponds reasonably to that of the parabolic stress distribution. The cone angle varies between $20° \leq \phi_D \leq 35°$ depending on the clamping length, bolt diameter, and edge distances [11]. A cone angle of $\phi_D = 30°$ is recommended if washers are used [12], and this value is adopted in this study.

2. Preload loss due to viscoplasticity

Viscoplastic behaviour of the bolt and the plates, as well as embedment creep, may cause preload loss over time. Embedment creep or embedment relaxation results from surface imperfections of threads, washers, and plates, even with a high rate of finish, [13]. The first contact points in the connection are highly stressed and plastic deformation occurs until a more or less stable situation is obtained when enough surface is used to prevent further plastic deformation, [14]. A large variation of relaxation is experienced, depending on the surface condition, finish, initial and local tension levels, and fit between the parts. Values for embedment creep per contact face reported for carbon steel depend on the surface roughness and range between $1.5\ \mu m \leq \varepsilon_{cr,em} \leq 6.5\ \mu m$ [11]. Yet, these small deformations can result in significant preload loss. Bickford [13] reports embedment creep related preload loss levels ranging between 5 and 10%. Chesson and Munse [15] report embedment creep related preload loss levels ranging between 2 and 11% for a specific bolt assembly (6-inch A325 bolt with two ¾-inch A7 steel plates). Values for embedment creep in a connection with aluminium plates are not reported. It is difficult to separate embedment creep from immediate elastic recovery and early viscoplastic relaxation of bolt and plates in practice. Theoretically, retightening of the bolt should neutralize embedment creep, because levelling of the surfaces is accomplished after embedment creep has occurred.

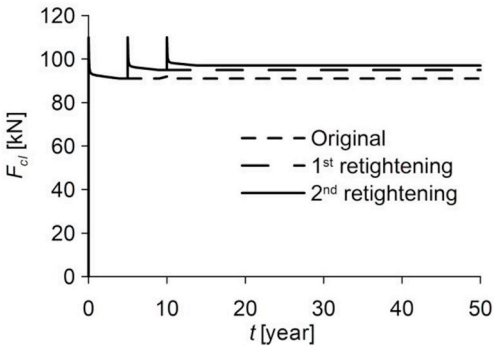

Fig. 2. Preload loss (excluding embedment creep) in a bolted connection with stainless steel bolts with retightening after 5 and 10 years, data from Ref. [18].

2.1. Relaxation of bolts

Shemwell and Johns [16] and Afzali et al. [8,17] carried out tests on carbon steel and stainless steel bolted connection assemblies. Preload losses at room temperature were observed for bolt stress levels exceeding 50% of the 0.2% proof stress. Tests where an initial preload force equal to the nominal value (Eq. (1)) was applied, showed a drop of preload directly following the tightening procedure that is mainly attributed to settlement and elastic recovery. Subsequent loss of preload followed a power function with time. This power function was calibrated to the measured data and subsequently applied to estimate the preload loss after 50 years. This provided an average preload loss between 6% and 10%, almost independent on the type of stainless steel (austenitic, ferritic, duplex or lean duplex) and comparable with that of carbon steel bolts and bolted connections. Relaxation of the plates appeared negligible, so that this preload loss could be attributed to relaxation of the bolt and nut. Hradil et al. [18] showed that retightening of bolts can reduce the preload loss due to relaxation of stainless steel bolts, but that the preload loss directly following the tightening procedure prevails, see Fig. 2. Note that embedment creep is not considered in Hradil's analysis and figure.

A creep model for bolts is developed here in order to extend Alfali's study of bolt relaxation to other geometries. Creep strain rates of the

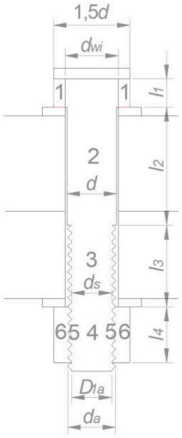

i	Description	A_i	l_i
1	Bolt head bearing	$\pi/4\left([1.5d]^2 - {d_{wi}}^2\right)$	$d/2$
2	Unthreaded shaft	A_d	$l_2 + d/2$
3	Threaded unegaged shaft	A_s	l_3
4	Threaded engaged shaft, per pitch j	$\frac{\pi}{4}\frac{{d_3}^2}{f_j}$	p
5	Interface bolt nut, per pitch j	$\frac{\pi}{4}\frac{{d_a}^2 - {D_{1a}}^2}{f_j}$	p
6	Nut bearing, per pitch j	$\frac{\pi}{4}\frac{[1.5d]^2 - {d_{wi}}^2}{f_j}$	p

Fig. 3. Decomposed bolt.

base metal are used as starting point for the model. Because creep strains of cold formed stainless steel base metal 316 (EN 1.4401) at room temperature has not been found in literature, test data in Refs. [19] for cold formed wire 304L (EN 1.4307) is used. The two alloys have similar tensile properties (difference less than 10%) and chemical composition (304L has a slightly higher chromium content, slightly lower nickel content, and no molybdenium). We used the general creep strain rate function of Eq. (3) and calibrated it with the test data. This function is also mentioned in Ref. [8] and a slightly modified version (and presented in a different shape) has successfully been applied to stainless steels in Ref. [19].

$$\dot{\varepsilon}_{cr} = f(\sigma)t^{-1} \tag{3}$$

where t is the time and σ is the stress. Following [20] the stress dependency function $f(\sigma)$ is calibrated with creep data using an exponential function for high stress ranges and a power function for low stress ranges:

$$f(\sigma_b) = \begin{cases} 1.53^{-32}\left(\dfrac{\sigma_b}{\mathrm{N/mm^2}}\right)^{10.1} & \text{if } \sigma_b \le 663\,\mathrm{N/mm^2} \\ 3.18{\cdot}10^{-4}\exp\left(4.11{\cdot}10^{-3}\dfrac{\sigma_b}{\mathrm{N/mm^2}}\right) - 4.39{\cdot}10^{-3} & \text{if } \sigma_b > 663\,\mathrm{N/mm^2} \end{cases} \tag{4}$$

where the value of 663 N/mm^2 is the intersection of the two equations.

The creep deformation of the bolt is determined as the summation of the deformations of the separate parts of the bolt assembly, see Fig. 3:

$$\Delta u_{cr,b} = \sum_i \varepsilon_{cr,i} l_i = \sum_i l_i \int_{t_0}^{t_e} \dot{\varepsilon}_{cr}\left(\frac{F_{cl}(t)}{A_i}\right) \mathrm{d}t \tag{5}$$

where subscript i denotes the separate parts of the bolt as distinguished in VDI 2230 (parts $1 \le i \le 3$ in Fig. 3) [11] or composed by the authors (parts $4 \le i \le 6$), with their bearing or tension area A_i, length l_i, and creep strain $\varepsilon_{cr,i}$. Time t_e is the intended life and time t_0 is the substitutional time reflecting the time involved in tightening.

The bearing area of the bolt head on the washer, A_1 in Fig. 3, and the corresponding substitutional extension height of the bolt head deformation, l_1, are taken from VDI 2230 [11]. The model of [21] is applied to estimate the fractions f_j of the total force transferred by pitch number j. Tolerance class 6 h is used together with the basic profile of a thread in ISO 68-1 [22] to establish the bearing diameter per thread, D_{1a}. A numerical procedure is required to solve Eq. (5), because the clamping force $F_{cl}(t)$ depends on the bolt relaxation deformation $\Delta u_{cr,b}$ through Eq. (2). Using this model, the preload loss ΔF_{cl} is determined for the bolt geometries of Afzali et al. [17], adopting the intended life of $t_e = 50$ y and the substitutional preload time $t_0 = 3$ s to exclude effects introduced during the tightening procedure. Table 1 compares the calculated preload loss with the extrapolation of the measurements in Ref. [17]. The table shows a reasonable agreement: the calculated values are on the higher end of the measured and extrapolated range.

Table 1
Calculated preload loss in 50 years compared to extrapolation of the measurements in Ref. [17].

Bolt diameter	$\Sigma T/d$	$F_{cl,nom}$	ΔF_{cl} extrapolation measurement	ΔF_{cl} calculation model
M16	3.7	88 kN	6.4–10.4 kN	9.1 kN
M20	3.75	137 kN	6.2–11.6 kN	11.8 kN

Table 2
Creep strain of aluminium alloys based on measurements in Ref. [23], and using Eqs. (3) and (6) with calibrated coefficients c_1 and c_2 as given in Fig. 4.

Alloy	σ_p/f_u [−] [a]	t [hr]	ε_{cr} [−] in [23]	ε_{cr} [−] Eq. (3),(6) [b]
5454-O	0.96	100	0.002	0.0018
5454-O	0.96	10	0.001	0.0016
5454-O	0.94	1000	0.010	0.0020
5454-O	0.92	1000	0.005	0.0020
5454-O	0.88	100	0.001	0.0017
5454-O	0.8	1000	0.002	0.0016
6061-T6	0.98	10	0.010	0.0092
6061-T6	0.98	100	0.010	0.0104
6061-T6	0.98	0.1	0.005	0.0069
6061-T6	0.96	1000	0.010	0.0064
6061-T6	0.96	10	0.005	0.0051
6061-T6	0.96	1	0.005	0.0045
6061-T6	0.96	0.1	0.002	0.0039
6061-T6	0.93	100	0.005	0.0035
6061-T6	0.93	100	0.005	0.0032
6061-T6	0.93	100	0.002	0.0032
6061-T6	0.93	10	0.002	0.0028
6061-T6	0.93	1	0.002	0.0025
6061-T6	0.93	10	0.001	0.0028
6061-T6	0.93	1	0.001	0.0025
6061-T6	0.93	0.1	0.001	0.0021
6061-T6	0.91	1000	0.002	0.0019
6061-T6	0.91	100	0.001	0.0017

[a] f_u = tensile strength, equal to 250 N/mm^2 and 310 N/mm^2 for alloys 5454-O and 6061-T6, respectively, [23].

[b] Coefficients $c_1 = 6.64 \times 10^{-13}$ and $c_2 = 3.74$ for alloy 5454-O and $c_1 = 9.65 \times 10^{-71}$ and $c_2 = 26.9$ for alloy 6061-T6.

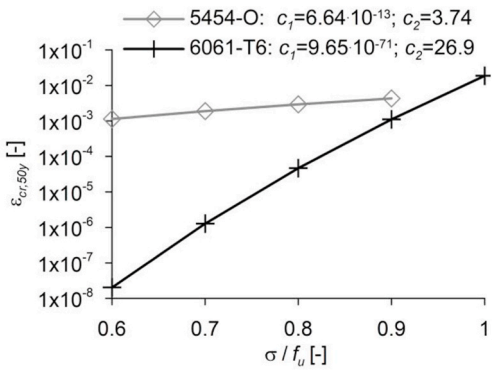

Fig. 4. Creep strain in aluminium alloy plates after 50 years of exposure to a constant stress, predicted with a creep model according to Eq. (6).

Table 3
Tensile properties of the materials in the experimental program according to their certificates (and between brackets the nominal values).

Material	Plate 5083-H111	Plate 5083-H111	Plate 5083-H111	Bolt 316 (A4 80)
Dimensions	T = 25 mm	T = 20 mm	T = 10 mm	M16-110 mm
$f_{0.2}$ [N/mm^2]	168 (125)	153 (125)	165 (125)	646 (600)
f_u [N/mm^2]	310 (275)	296 (275)	287 (275)	867 (800)

2.2. Creep of aluminium alloys

Room temperature creep rates of aluminium alloys may be higher as compared to that of carbon steel and stainless steel. Consequently, plate creep may not be negligible in bolted connections with aluminium plates. Kaufmann [23] reports creep rates of aluminium alloys at various constant temperatures and holding times up to 1000 h. Instead of data from individual tests, the interpretation thereof is provided as the stress level resulting into certain creep strain after a certain holding period. It is unknown how many creep tests have served as a basis for the values reported. Data are not reported for alloy 5083-H111, but the differences in creep rates between alloys in the same series in the same temper and with similar 0.2% proof stress appears small. Creep data of alloy AA 5454-O are therefore used here. The latter alloy has a lower magnesium content as the former (2.4–3.0 versus 4.0–4.9 weight percent), whereas the contents of other elements are equal. A stronger alloy, AA 6061-T6, is also considered for reasons of comparison. The general creep Eq. (3) is adopted with a power equation to express the sensitivity of the creep strain rate, $\dot{\varepsilon}_{cr}$, on the stress level in the plates, σ_p:

$$f(\sigma_p) = c_1 \left(\frac{\sigma_p}{\mathrm{N/mm^2}} \right)^{c_2} t^{-1} \tag{6}$$

coefficients c_1 and c_2 are calibrated so as to give the best match with the creep data in Ref. [23], see Table 2. Fig. 4 gives the values for calibrated coefficients c_1 and c_2 and the resulting creep strain developed after 50 years of constant stress. The coefficient of determination of the relationship is R^2 = 0.34 and 0.89 for alloys 5454-O and 6061-T6, respectively. Hence, the coefficient of determination of alloy 5454-O is low, and the number of data is small. Other general creep functions than Eq. (6) developed for low temperature creep of metals collected in Ref. [19] did not give a better agreement with the data. Despite the lack of accuracy, it is clear – and expected – that alloy 5454-O is subjected to significantly higher creep strains at low relative stress levels as compared to alloy 6061-T6.

Because of the uncertainty related to creep of the 5xxx series aluminium alloys in soft temper, we performed a limited number of exploratory creep tests on base material. Almost cubic samples (28 × 28 × 25 mm^3) were cut from a 25 mm thick base plate of alloy 5083-H111, with tensile properties according to Table 3. Four of these cubes were staggered and loaded in an Instron hydraulic test machine. The load was

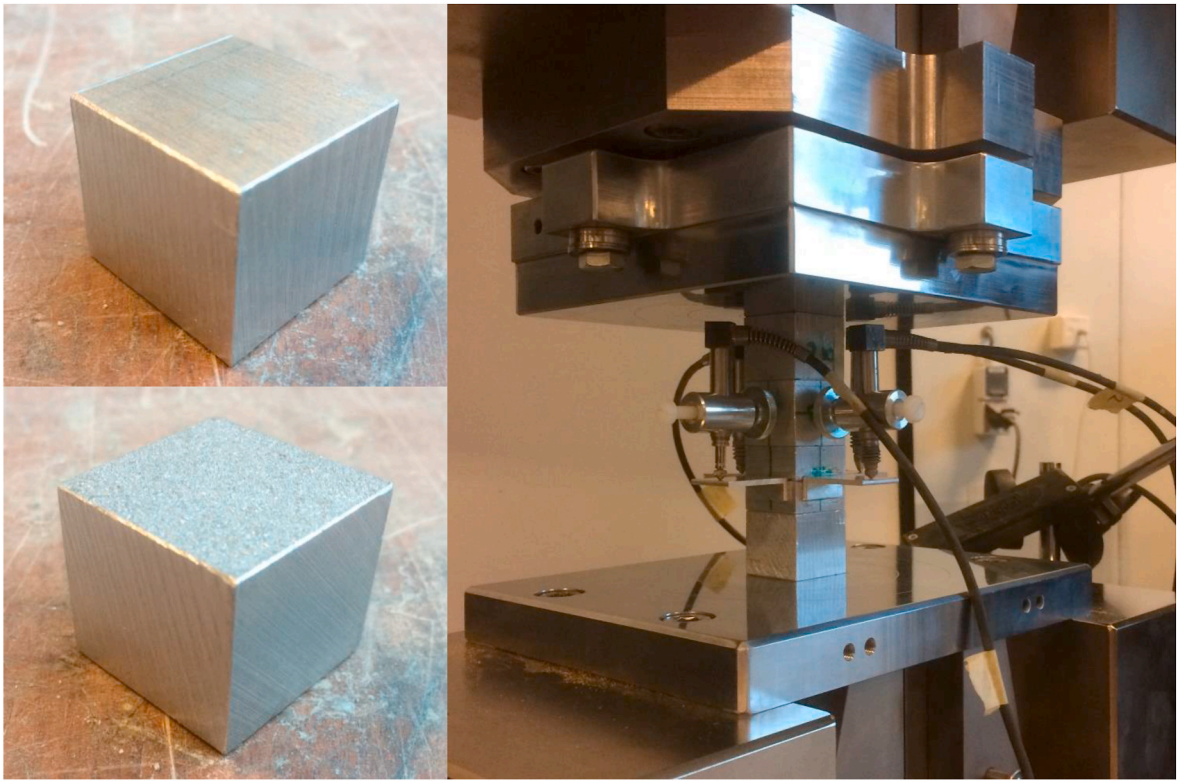

Fig. 5. Creep tests applied to cubes of aluminium alloy 5083-H111 with as-delivered (top left) and grit blasted (bottom left) surfaces.

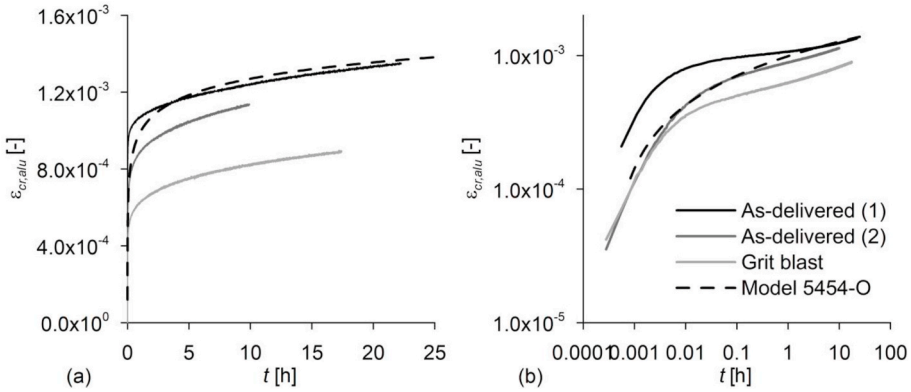

Fig. 6. Creep strain developed in the aluminium alloy 5083-H111 staggered cubes at a stress level of $\sigma_p = 241$ N/mm^2 (load remains constant at $t = 0$): (a) linear scale; (b) lognormal scale.

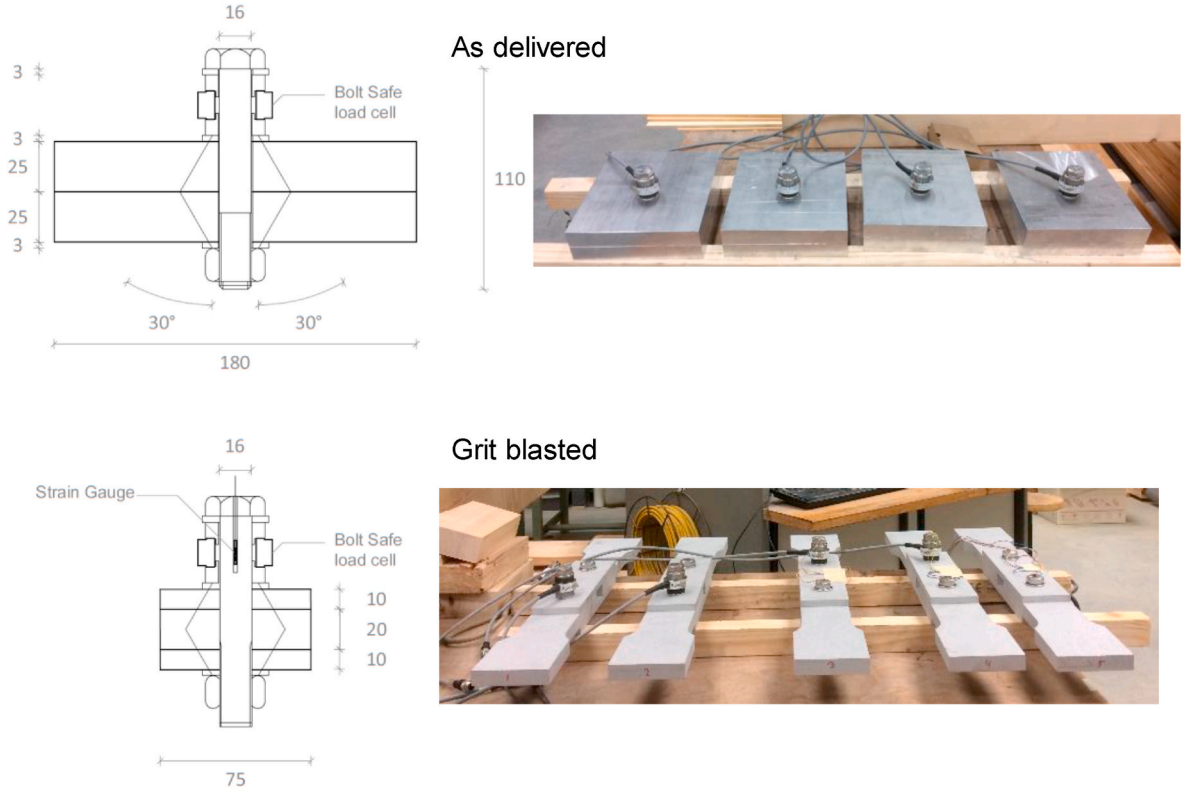

Fig. 7. Geometry of the specimen in the combined creep and relaxation tests.

selected in such a way that the stress in the specimen corresponded to that of the bearing stress in the plate material just below the washers of an M16 bolt that is preloaded to $F_{cl,nom}$. This stress level is $\sigma_p = 241$ N/mm^2. The load was applied in 2.5 min with a constant deformation rate and subsequently kept constant for 10–22 h. LVDT-s were used to measure the deformation between the centres of the two centre cubes, i.e. with a measuring distance of 25 mm and one cube interface in between. Two tests were performed with as-delivered specimen and one test with specimen with a grit blasted surface. The latter had a measured mean roughness of $R_a = 15$ μm.

Fig. 5 gives the set-up of the aluminium base material creep tests. Fig. 6 presents the measured strain while the force remained constant. The majority of creep deformation occurs within the first 2 h after application of the load. The specimen with blast surface showed less creep deformation as compared to the other specimen, but this specimen showed larger deformation during application of the load. The figure also provides the calculated creep strain using the model of alloy 5454-O, which was determined under the assumption of $t_0 = 3$ s, in agreement with [8], and $\varepsilon_{cr,em} = 3$ μm, in agreement with [11]. Note that the creep developing in the first seconds is relatively sensitive to the choices of t_0 and $\varepsilon_{cr,em}$.

As commonly observed in creep tests, e.g. Ref. [24], the creep strain is significantly scattered, which is demonstrated by the difference in creep strain between the tests with equal conditions. Given this scatter, the simple Eq. (6) calibrated with the data of alloy 5454-O reasonably predicts the creep strains, i.e. the model provides the correct order of magnitude of the creep strain, which is the aim of the current study.

2.3. Combined creep and relaxation of a bolted connection

Combined creep and relaxation tests were subsequently performed on bolted connections with stainless steel M16 110 mm long bolts and

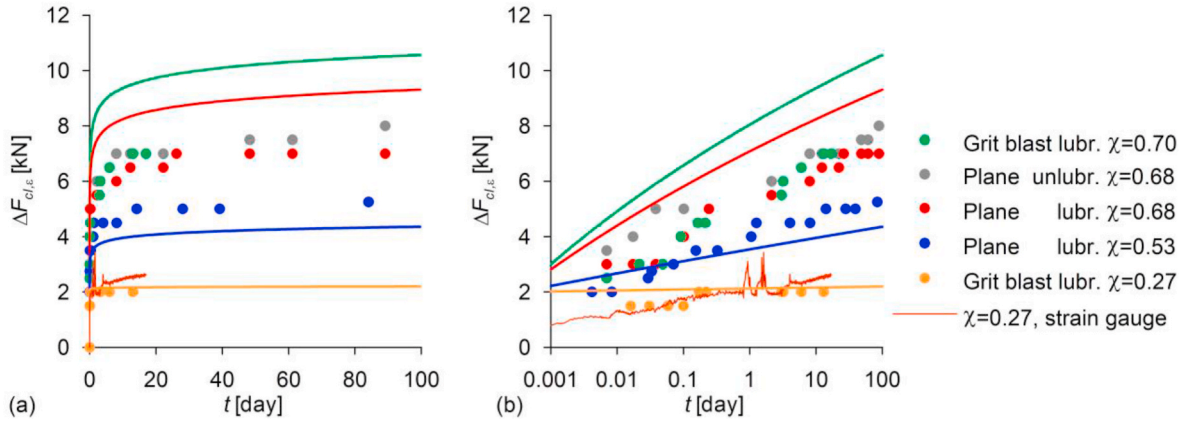

Fig. 8. Creep and relaxation tests of bolted connections (plates 5083-H111. $\Sigma T = 40$ mm, bolt 316 (A4 80), 110 mm): (a) Linear scale; (b) Lognormal scale.

aluminium alloy 5083-H111 plates. Tensile properties are listed in Table 3. Tests were performed with two as-delivered plates with a thickness of 25 mm, and with three grit blasted plates with thicknesses of 10, 20 and 10 mm. The bolts were instrumented with BoltSafe CMS load cells, Fig. 7, that were calibrated before testing. These load cells are designed especially for long-term monitoring of bolt loads, showing practically no creep deformation. The combined height of the load cell and its adapter rings is 30.3 mm and the associated, approximate spring stiffness is $k_{lc} = 2217$ kN/mm. The bolts were preloaded to fractions of the nominal tensile strength of the bolt ranging between $0.27 \leq \chi \leq 0.70$ (where $\chi = F_{cl}/(A_s f_{ub})$) and each test was repeated at least 4 times. Nyloc nuts were used. The threads of the bolts were lubricated with Hytorc HY52 Paste White, which is designed for reduced probability of frictional corrosion to the aluminium plates or stainless steel bolts. A small number of test series was repeated without lubricant in order to determine its influence on preload loss. The average torque required for preloading the bolt to the nominal clamping force ($\chi = 0.70; F_{cl,nom} = 88$ kN) was 180 Nm and 450 Nm for the lubricated and non-lubricated bolts, respectively. The coefficient of variation of the clamping force was 8% at these torques for both cases.

The specimens were stored during 90 days in a climate room with a controlled, constant temperature of 20 °C and a constant relative humidity of 60%. The dots in Fig. 8 provide the average preload loss measured in the tests. One bolt in a test with $\chi = 0.27$ was equipped with a strain gauge applied in the core of the bolt. The strain gauge was calibrated before the test by loading the bolt in an Instron test machine and comparing the measured strain with the applied load. The dark brown curve in Fig. 8 represents the result of the strain gauge measurement during the creep and relaxation test. The spikes in this figure are caused by opening of the door of the climate room, giving a deviation of the temperature for a short period of time. These spikes are further ignored. Preload loss determined with the load cells (yellow dots in Fig. 8) agrees with that of the strain gauge (dark brown curve). The other curves are introduced later.

Fig. 8 demonstrates that relaxation increases with increasing preloading level χ (as expected). It also shows that the unlubricated specimen provide a marginally larger preload loss as compared to the lubricated specimen and that the grit blasted specimen provide approximately equal preload loss as compared to the as-delivered specimen.

The stresses and strains in the plates of a bolted connection can be approximated with the VDI 2230 stress frustum model of Fig. 1, under the following assumptions:

- The creep relation as determined for tension action also applies to compression;
- The cone is a stand-alone part, i.e. not connected to the remainder of the plates;
- The stress state in the cone can be approximated as a uniaxial stress.

The stress as a function of height and time, σ_p, and the deformation caused by plate creep, $\Delta u_{cr,p}$, then follow from:

$$\sigma_p(z,t) = \frac{-F_{cl}(t)}{\frac{\pi}{4}\left((1.5d + 2T_w \tan\phi_D + 2z\tan\phi_D)^2 - d_0^2\right)} \tag{7}$$

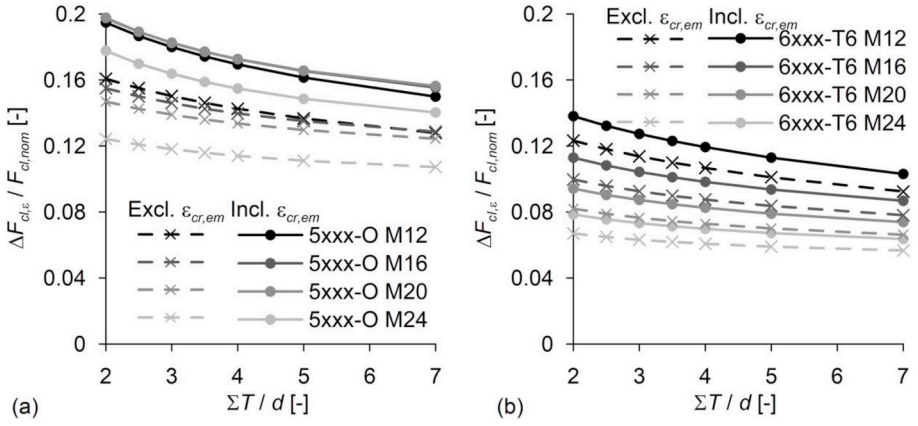

Fig. 9. Parametric study into preload loss after 50 years caused by viscoplastic behaviour for a nominal initial preload force: (a) Alloys 5454-O/H111 and 5083-O/H111; (b) Alloy 6061-T6.

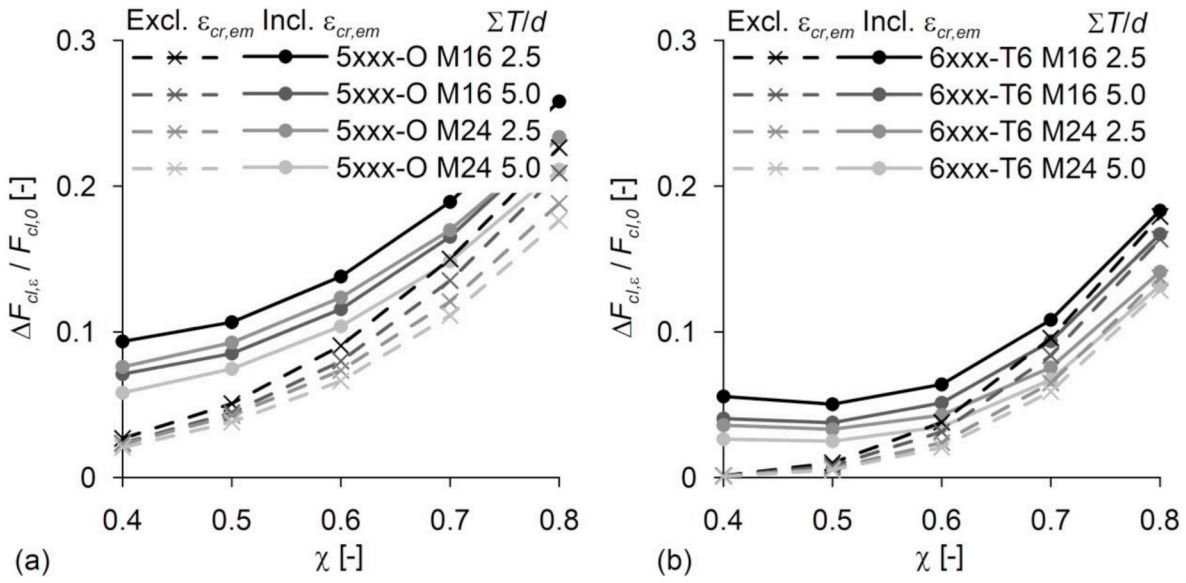

Fig. 10. Parametric study into preload loss after 50 years caused by viscoplastic behaviour for different initial preload forces: (a) Alloys 5454-O/H111 and 5083-O/H111; (b) Alloy 6061-T6.

$$\Delta u_{cr,p} = -2 \int_0^{\frac{\sum T}{2}} \int_{t_0}^{t_e} z \dot{\varepsilon}_{cr,alu}(\sigma_p) \mathrm{d}t \mathrm{d}z \tag{8}$$

where d and d_0 are the bolt and bolt hole diameter, respectively, $\sum T$ is the thickness of the plate assembly, T_w is the washer thickness, and z is the height as indicated in Fig. 1.

Eqs. (2) and (5)-(8) are used to estimate the preload loss due to relaxation of the bolt and creep of the plates. The elastic spring stiffness is used in Eq. (2), because viscoplastic material behaviour is assumed and hence the elastic stiffness applies in case of unloading. The continuous curves in Fig. 8 provide the calculated preload loss for $t_0 = 30$ s, reflecting the assembly time, and $\varepsilon_{cr,em} = 9\ \mu m$, in agreement with [11] for three interfaces. The model predicts a too large preload loss at high preload levels ($\chi \geq 0.68$) and too small preload loss at low preload levels ($\chi \leq 0.53$). However, the model provides the correct order of magnitude of the creep strain. For the more relevant case of high preload levels, the model predicts on average a preload loss after 10 min that is 43% higher and a subsequent rate of preload loss that is 14% higher as compared to the average of the tests. These differences between the tests and the model will be considered later in this paper. The prediction is sensitive to the choices of t_0 and $\varepsilon_{cr,em}$. This also reflects the importance of the assembly time in practical applications and the application or not of retightening: a relatively long assembly time reduces preload loss through relaxation and retightening reduces the impact of embedment creep.

We used the model to estimate the preload losses due to viscoplastic behaviour, $\Delta F_{cl,\dot{\varepsilon}}$, for geometries different than the tested ones. Fig. 9 provides the relative preload loss at the end of 50 years in service for M12 up to M24 stainless steel bolts that are preloaded to the nominal value and applied in a connection with relative plate thickness varying between $2 \leq \Sigma T/d \leq 7$. Following standard practice for civil structures, the hole diameter, d_0, was selected as $d_0 = d + 1$ mm for bolt M12 and $d_0 = d + 2$ mm for bolts M16, M20 and M24. The dashed curves provide the preload loss if embedment creep is not considered while the continuous curves provide the preload loss including embedment creep of 9 μm for the entire connection. The figure demonstrates a significant

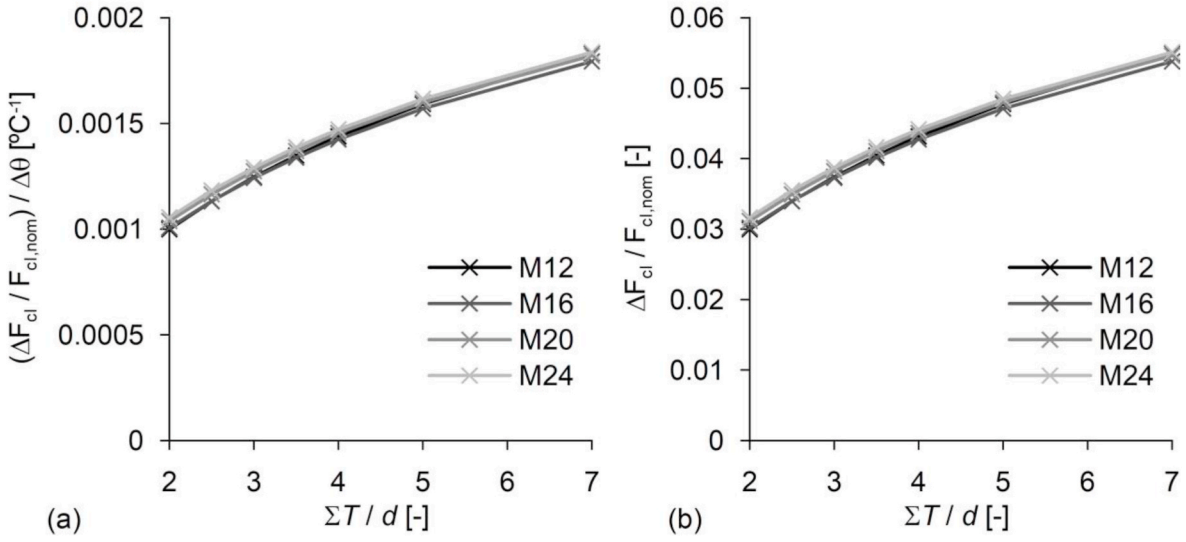

Fig. 11. Parametric study into preload loss due to temperature variations: (a) Relative preload loss per unit temperature variation; (b) Relative preload loss for $\delta\theta = 30$ °C.

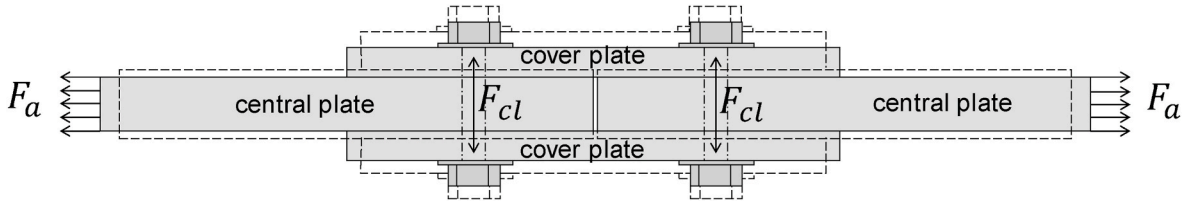

Fig. 12. Schematic presentation of preload loss due to lateral contraction.

preload loss in 50 years due to viscoplastic behaviour of stainless steel bolts and aluminium plates: between 5% and 18% of the original value. A lower preload loss is predicted for larger grip lengths. In addition, the figure demonstrates a 1.4 up to 2 times larger predicted preload loss for alloys 5083-O/H111 or 5454-O/H111 as compared to alloy 6061-T6. Plate creep of alloy 6061-T6 in the connection appears negligible and hence, the displayed preload loss is fully caused by bolt relaxation. Fig. 10 provides the relative preload loss after 50 years for M16 and M24 bolts, $\Sigma T/d = 2.5$ and 5, for different initial preload forces. The initial preload force appears to significantly influence the preload loss.

3. Preload loss caused by thermal action

Temperature variations may result in preload variations, because the coefficient of linear thermal expansion of stainless steel, α_b, is different from that of aluminium, α_p. The coefficient of linear thermal expansion of aluminium is almost independent of the alloy and equal to $\alpha_p = 23{\cdot}10^{-6}\,{}^{\circ}C^{-1}$ [25], whereas the value for stainless steel depends on the grade and varies between $9{\cdot}10^{-6}\,{}^{\circ}C^{-1} \leq \alpha_b \leq 18{\cdot}10^{-6}\,{}^{\circ}C^{-1}$. The value for stainless steel alloy 316 (1.4401) is $\alpha_b = 16{\cdot}10^{-6}\,{}^{\circ}C^{-1}$ [26]. The relative deformation, Δu, in case of a temperature variation, $\Delta\theta = \theta_t - \theta_0$, is equal to:

$$\Delta u = \Delta\theta(\alpha_b - \alpha_p)\Sigma T \tag{9}$$

The corresponding preload loss due to thermal action, $\Delta F_{cl,\theta}$, is determined through Eq. (2). The model is used in a parametric study. Fig. 11 gives the preload loss for stainless steel bolts with aluminium plates. The preload loss increases for increasing plate thickness. Small variations between different bolt types exist because of deviating stiffness ratios between bolt and plate assemblies due to differences in the thickness of washers. The preload loss at a temperature that is 30 °C lower than during assembly is approximately 5% for $\Sigma T/d = 5$. This effect is significant, but smaller than the preload loss due to viscoplastic material behaviour.

4. Preload loss caused by lateral contraction

Lateral contraction of the plates occurs if an external load is applied to the connection. An external tensile load will therefore result in preload loss, see Ref. [27] and Fig. 12. A multiaxial stress state occurs in the plate material due to the combination of the external load and bolt preload. The material may be subject to stress exceeding the yield limit close to the washers.

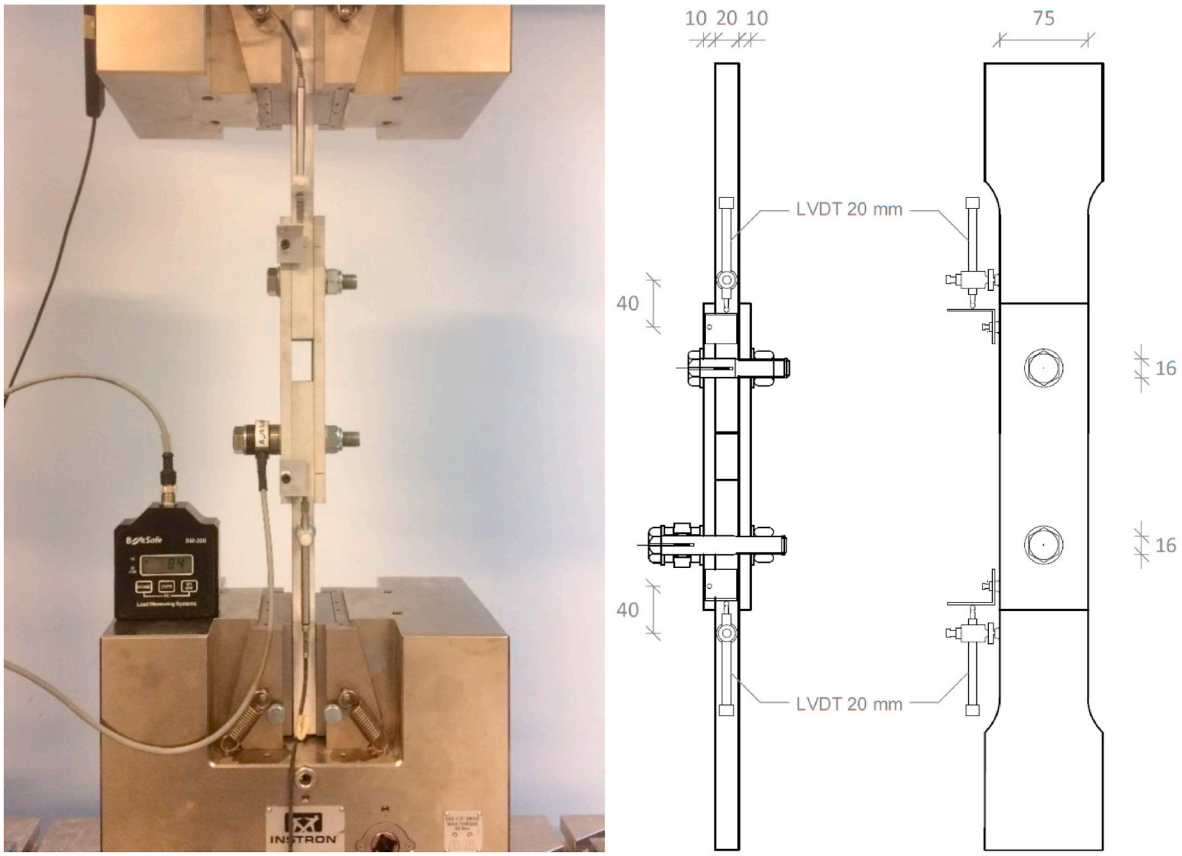

Fig. 13. Test set-up and specimen for the lateral contraction tests.

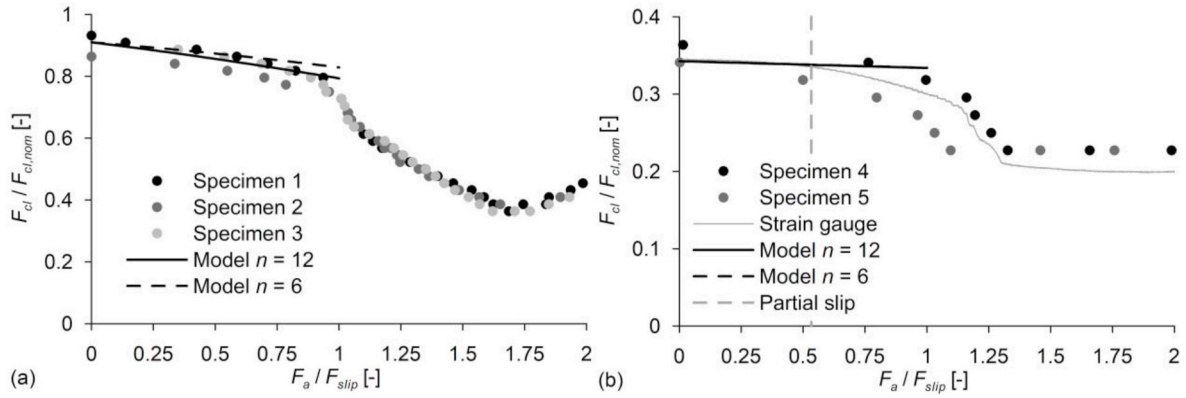

Fig. 14. Results of the lateral contraction tests and comparison with the model: (a) Results for three tests carried out at a high preload level; (b) Results for two tests carried out at a low preload level.

4.1. Model description

The yield locus of aluminium is often described with the Von Mises criterion and the Ramberg Osgood relation [27] is often used to describe the non-linear stress-strain relationship of aluminium [28,29]:

$$\varepsilon = \frac{\sigma}{E} + 0.002\left(\frac{\sigma}{f_{0.2}}\right)^n \tag{10}$$

where E is Young's modulus and n is the hardening exponent. Considering incompressibility of material in plastic state, the model can be extended to a multi-axial stress state [30]:

$$\boldsymbol{\varepsilon} = \boldsymbol{\varepsilon}_{\mathbf{el}} + \frac{3}{2}\frac{0.002}{(f_{0.2})^n}(\sigma_{VM})^{n-1}\cdot\boldsymbol{S} \tag{11}$$

where $\boldsymbol{\varepsilon}_{el}$ is the elastic strain tensor and $\boldsymbol{S}$ is the deviatoric stress tensor. For the current application, the strain in the plates in the direction of preloading, ε_p, results from the stress caused by the preload, σ_p, and the applied stress, σ_a, working in orthogonal directions. Eq. (11) then reduces to:

$$\varepsilon_p = \frac{\sigma_p}{E} - \frac{\nu\sigma_a}{E} + \frac{3}{2}\frac{0.002}{(f_{0.2})^n}\left({\sigma_p}^2 + {\sigma_a}^2 - \sigma_p\sigma_a\right)^{\frac{n-1}{2}}\cdot\left(\sigma_p - \frac{1}{3}\left[\sigma_p + \sigma_a\right]\right) \tag{12}$$

where ν is the Poisson ratio. The stress caused by preloading, σ_p, can be determined with the frustrum model of Eq. (7). Assuming that the applied stress is equally distributed over the various plates in the assembly at the location of the bolt, the stress caused by the external action, σ_a, can be determined with:

$$\sigma_a = \frac{F_a}{(w - d_0)\Sigma T} \tag{13}$$

where w is the width of the plates and F_a is the applied load. The relative connection deformation caused by lateral contraction can be determined with:

$$\Delta u = 2\int_0^{\frac{\sum T}{2}}(\varepsilon_p - \varepsilon_o)dz \tag{14}$$

where ε_o = strain in length direction of the plate(s) without an applied load, i.e. Eq. (12) with $\sigma_a = 0$.

Resulting preload loss due to lateral contraction, $\Delta F_{cl,\nu}$, can again be determined with Eq. (2). Linear elastic spring stiffness can again be used in Eq. (2) as the plates are unloaded in direction of the preload.

Table 4
Tensile test properties used in the simulations for lateral contraction.

Alloy	ν (−) [a]	E (N/mm^2) [a]	$f_{0.2}$ (N/mm^2)	n (−) [a]
5083-H111	0.33	72000	165 [b]	12 [d]
6061-T6	0.33	69000	275 [c]	30

[a] Values origin from tests on other batches of the same ally and temper carried out in our laboratory, except for data assigned with b) or c).
[b] Value origins from the material certificate.
[c] Value origins from Refs. [23].
[d] The model is also applied with the nominal value $n = 6$ [32] to study its influence.

4.2. Tests on lateral contraction

The model constituting Eq. (2), (10)–(14) is checked by comparing the results with tests. A tensile load was applied to the grit blasted specimen that were first subjected to combined creep and relaxation, the latter described in Section 2. Fig. 13 shows the specimen and test set-up. M16 bolts were applied in holes with $d_0 = 17$ mm. The width of the plate was $w = 75$ mm, the plate thickness, T, were 20 mm and 10 mm for the central plate and the cover plates, respectively, see the bottom left graph of Fig. 7. The tests were performed in controlled deformation in an Instron test machine. Preload loss was determined with BoltSafe CMS load cells and, for the bolts with low preloads, also with strain gauges. In addition, linear variable differential transformers (LVDT-s) were applied between the central plate and the edges of the cover plates to detect slip between the plates.

The friction coefficient was estimated from the applied load at the occurrence of full slip as detected with the LVDT-s. The average friction coefficient was $\mu = 0.75$. The LVDT-s detected a non-linear force-displacement relationship before the connection fully slipped. This is attributed to slip of those parts of the connection that are not in the direct vicinity of the bolt and hence subject to lower than average pressure between the plates. This is further referred to as partial slip. The slip load, F_{slip}, is defined as:

$$F_{slip} = m\mu F_{cl} \tag{15}$$

where m is the number of contact planes ($m = 2$). The dots in Fig. 14 represent the load cell measurements and the purple curve represents the strain gauge measurement of one of the bolts. Four other specimen equipped with strain gauges but without a load cell showed a similar behaviour. These are not shown.

The measuring data show a steady decreasing preload force up to the attainment of the slip load and after that a rapidly decreasing preload. At a very large load, i.e. much larger than the slip load, the preload increases again. This is attributed to thickening of the plates at the hole perimeter due to bearing of the bolt [27], and to bending of the bolt so

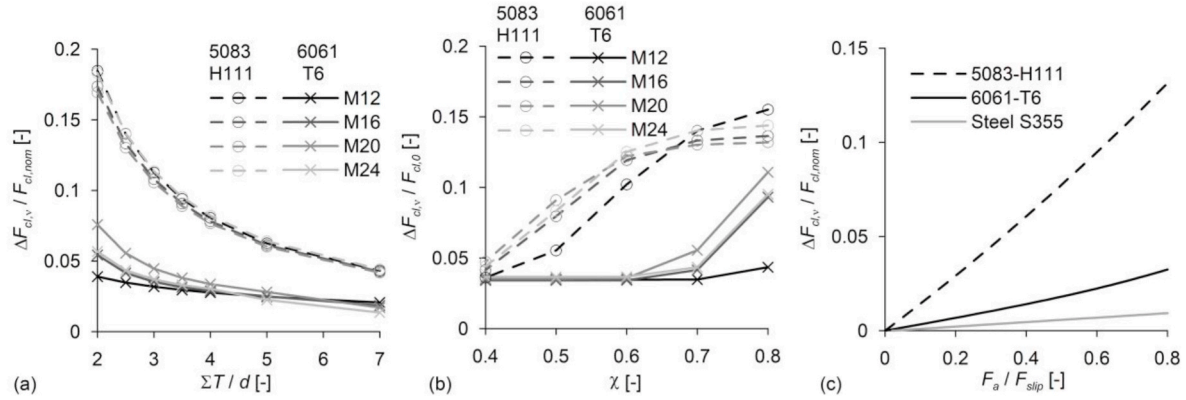

Fig. 15. Parametric study into preload loss due to lateral contraction with $w = 2.4d_0$ and $\mu = 0.4$: (a) Results for different plate thickness with $\chi = 0.7$ and $F_a = 0.8F_{slip}$; (b) Results for different preload ratios with $\Sigma T/d = 2.5$ and $F_a = 0.8F_{slip}$; (c) Results for different applied loads, M16 bolts with $\Sigma T/d = 2.5$ and $\chi = 0.7$.

that the edges of the bolt head and nut make contact with the plates, [31]. The trajectory up to full slip is relevant for the current study.

The red curves in Fig. 14 provide the results of the model comprising Eqs. (2) and (10)-(14), using the 0.2% proof stress of the cover plates according to the certificate (Table 3): $f_{0.2} = 165$ N/mm^2. The Ramberg Osgood exponent, n, is not provided in the certificate. An average value of $n = 12$ is selected from tests carried out in our laboratory on other batches of alloy 5083-H111. As the value is uncertain, the model is also applied with the nominal value $n = 6$ according to Ref. [32] in order to determine the sensitivity of the preload loss on the exponent value. The other relevant material properties applied in the model are also based on tests in our laboratory on other batches of this alloy, and are listed in Table 4. Comparing the red curves and the experimental data in Fig. 14 reveals a good agreement in case of large preload levels and the model with $n = 12$ (Fig. 13a). A good agreement is also obtained between this model and the tests with low preload level, but then only up to the load at which partial slip was detected (Fig. 13b).

4.3. Simulations of preload loss due to lateral contraction

The model is used to evaluate the preload loss, $\Delta F_{cl,v}$, in connections with various dimensions in a parametric study. The preload loss resulting from lateral contraction implies that the theoretical slip load from Eq. (15) using the initial preload force, i.e. $F_{cl} = F_{cl,0}$, cannot be obtained. For this reason, standards apply a safety factor for slip. The preload loss is therefore determined at 80% of the theoretical slip load, i.e. considering a safety factor of 1.25. The ratio between applied stress and slip load, and therefore the preload loss resulting from lateral contraction, increases for decreasing plate dimensions, see Eq. (13). The simulations are therefore performed for a plate width of $w = 2.4d_0$, which is the smallest width allowed in the European standard for aluminium structures, EN 1999-1-9 [32]. A friction coefficient of $\mu = 0.4$ is applied, equal to the nominal value in Refs. [32] for grit blasted surfaces. Fig. 15a and (b) give the results of the simulations, for various thickness, initial preload levels, and for two alloys with tensile test properties according to Table 4.

Fig. 15 (a) and (b) reveal a substantial preload loss especially for alloy 5083-H111 and relatively thin plates. The difference between the alloys is mainly related to the difference in $f_{0.2}$. However, the preload loss remains below 20% for all cases considered, implying that the connection is able to transfer the applied load $F_a = 0.8F_{slip}$. Fig. 15c gives a comparison at different applied load levels for one specific geometry and initial preload force. In addition to the two aluminium alloys, a steel grade is considered with a yield stress of 355 N/mm^2, Young's modulus of 210000 N/mm^2, and a Poisson ratio of 0.3. The preload loss at $F_a = 0.8F_{slip}$ is 1%, 3%, and 13% for the steel grade, alloy 6061-T6, and alloy 5083-H111, respectively. The lower preload loss for the steel case origins from the higher modulus of elasticity, lower Poisson ratio, and higher yield strength as compared to the aluminium alloys.

5. Discussion

5.1. Measures to minimise preload loss

The parametric studies of the previous sections demonstrate that the preload loss in aluminium plated slip resistant connections can be substantial. The main sources are relaxation of bolts and lateral contraction of the loaded plates. However, the preload loss can be limited by considering design options and preload procedures. A first option consists of retightening the bolts. This has limited influence on bolt relaxation in service, but it reduces embedment creep directly after tightening. If the connection is loaded in tension by the permanent load, retightening while in service reduces the preload loss due to lateral contraction. Slow tightening of bolts is also beneficial to limit embedment creep and relaxation, because the major part of preload loss due to relaxation occurs in the first seconds after tightening. Third, preload loss due to relaxation can be limited by applying a grip length that is not too small, e.g. $l_g/d \geq 3$. In practice, this can be achieved through applying bushings or increasing the thickness of the cover plates. The latter option has the additional advantage that it reduces preload loss due to lateral contraction, because it reduces the applied stress in the cover plates. Note that the non-linear effect of lateral contraction on the preload loss is entirely caused by the cover plates, which receive a high stress directly below the washer. To further limit the preload loss due to lateral contraction, it is advised to apply a minimum width of the plates, i.e. to design with the "standard" edge distance of $1.5d_0$ instead of the minimum value of $1.2d_0$, both values as specified in the standard EN 1999-1-1 [32].

This study has demonstrated that preload loss due to plate relaxation and lateral contraction is particularly large in case of alloys with low 0.2% proof stress. EN 1999-1-1 [32] limits the application of preloaded bolted connections to plate material with $f_{0.2} \geq 200$ N/mm^2. Reason is to limit plasticity in the plates that are in contact with the washers. This study shows that preload loss in case of plates with $f_{0.2} = 165$ N/mm^2, i.e. 18 % lower than the limit in Ref. [32], is already significant. On the other hand, contrary to the general specification in Ref. [32], a minimum proof stress is only relevant for the plates highly loaded through bolt preloading, i.e. the plates that are in contact with the washers. A lower proof stress of approximately $f_{0.2} = 125$ N/mm^2 may be allowed for the central plates, provided the cover plates are not too thin.

5.2. Reliability and partial factor

EN 1999-1-1 [32] provides the following design equation for the slip force of a connection with aluminium plates and carbon steel preloaded bolts:

$$F_{slip,d} = \frac{m\mu_c F_{cl,nom}}{\gamma} \tag{16}$$

where μ_c is the characteristic value of the friction coefficient, equal to $\mu_c = 0.4$ for aluminium-to-aluminium, grit blasted surfaces, and γ is the partial safety factor, equal to $\gamma = 1.25$ or 1.10 for slip resistant connections in the ultimate limit state (ULS) or serviceability limit state (SLS), respectively. It is now of interest to determine if this design model meets the required reliability in case of the current configuration with a stainless steel bolt, considering the preload losses and the uncertainties in the initial preload force and the friction coefficient.

Following EN 1990 [33] and ISO 2394 [34], resistance models should meet a required reliability of $\alpha_R\beta_{tar}$, where α_R is the first order reliability method (FORM) sensitivity factor for the resistance and is specified as $\alpha_R = 0.8$ in absence of detailed load information, and β_{tar} is the required reliability index with values $\beta_{tar} = 3.8$ and 1.5 for a reference period of 50 years and for the ULS and the SLS, respectively. The reliability index, β, is defined as:

$$P_f = \Phi(-\beta) \tag{17}$$

where P_f is the probability of failure and Φ is the cumulative distribution function of the standard normal distribution.

The reliability analysis performed here comprises of a connection for which a relatively large preload loss is expected. The lay-out of the connection is as in Fig. 12. A stainless steel bolt M16 with $f_{0.2} = 600$ N/mm^2 and preloaded with the torque method is applied in an aluminium plate assembly with $\Sigma T/d = 2.5$, where the cover plates are 10 mm thick and the central plate is 20 mm thick. The plate width is $w/d_0 = 2.4$, i.e. using the minimum edge distance of [32]. The hole diameter $d_0 = d + 2$ mm. The aluminium alloys have an 0.2% proof stress of $f_{0.2} = 200$ N/mm^2 and a Ramberg-Osgood exponent of $n = 15$. In the design point, the applied load is the dominant action and equal to the design value of the resistance. The actions are applied after 50 years in service, i.e. after maximum preload loss caused by creep and relaxation. A combination value applies to the thermal action, resulting into $\Delta\theta = 20\,^{\circ}C$. The limit state function, g, is defined as:

$$g = m\widehat{\mu}\left(\widehat{\chi} f_{ub} A_t - \widehat{C}\Delta F_{cl,\dot{\varepsilon}} - \Delta F_{cl,\theta} - \Delta F_{cl,\nu}\right) - F_{slip,d} \tag{18}$$

where symbols with circumflex represent the random variables. Random variable $\widehat{C}$ accounts for the uncertainty in the extrapolation of creep strain from measured periods to the reference period, the bias in the relaxation model, and the aleatoric variation of creep of individual specimen. The preload losses $\Delta F_{cl,\dot{\varepsilon}}$ and $\Delta F_{cl,\nu}$ are calculated using the equations in the previous sections based on the available preload at the time of application and they are therefore depending on the other random variables. Embedment creep is again considered through a relative deformation of 9 μm. The failure probability is determined as:

$$P_f = P(g < 0) \tag{19}$$

The distributions of the random variables are obtained from literature, or from expert opinion if literature is not available. EN 1090-2 [3] requires a tightening torque for carbon steel high friction grip bolts that results in a mean initial preload force that is 10% larger than the nominal value, i.e. $M_\chi = 0.77$. EN 14399-3 [35] and EN 14399-4 [36] require a coefficient of variation (V) of the ratio between applied torque and resulting clamping force of maximum 10%. EN 14399-2 [37] provides requirements on the testing tools that result in a V of maximum 2% and EN 1090-2 [3] requires a V of maximum 4% for torque tools applied in practice. EN 1090-2 [3] assumes that the previously mentioned variables are normal distributed. The resulting standard deviation of the preload ratio, χ, is then $S_\chi = 0.77\sqrt{0.10^2 + 0.04^2 + 0.02^2} = 0.09$. These values apply to carbon steel bolts in steel plate assemblies. Our study demonstrated that a similar standard deviation can be obtained for stainless steel bolts in aluminium plate assemblies, see Section 2.

The friction coefficient between aluminium-to-aluminium grit blasted surfaces is relatively uncertain. We have not found a comprehensive study that provides a distribution based on measured values. Therefore, based on our own experience and by consulting an expert, we estimated that the friction coefficient varies between 0.5 and 0.8 as 5% and 95% fractions. Galling may increase the friction coefficient, but the required relative movement to fully activate galling is larger than the hole clearance and it is therefore not considered. The resulting distribution for the friction coefficient has $M_\mu = 0.65$ and $S_\mu = 0.1$ as estimators.

Lognormal distributions are considered for uncertainty factors in Ref. [38,39], and we applied this for the uncertainty factor for viscoplastic behaviour. A comparison between the model prediction and the tests results in Section 2 (Fig. 8) gives $M_C = 0.91$ and a V of 0.19 for the ratio between tested and predicted preload loss due to relaxation after 100 days. An additional uncertainty with a V of 0.10 is considered to account for the extrapolation, i.e. the difference between the relaxation test duration and the reference period of 50 years. The combined standard deviation is $S_C = \sqrt{ln(0.19^2 + 1) + ln(0.10^2 + 1)} = 0.21$. Table 5 gives an overview of the random variables.

Eq. (19) is evaluated with the first order reliability method. The resulting reliability indices are $\beta = 1.70$ and $\beta = 2.35$ for $F_{slip,d}$ determined in SLS and in ULS, respectively. The reliability is larger than the required value $\alpha_R\beta_{tar}$ in SLS, but smaller in ULS. Fig. 16 provides the calculated reliability index, β, as a function of the partial factor, γ, in Eq. (16). It follows from this figure that the required reliability is met for $\gamma = 1.0$ and $\gamma = 1.5$ in SLS and in ULS, respectively.

Table 5
Distributions of the random variables applied in the FORM analysis.

Variable	Description	Distr.type	M_x	S_x	Nominal
$\widehat{\chi}$	Ratio between initial preload and nominal tensile strength	normal	0.77	0.085	0.7
$\widehat{\mu}$	Friction coefficient	normal	0.65	0.10	0.4
$\widehat{C}$	Model uncertainty for relaxation	lognormal	0.91	0.21	1.0

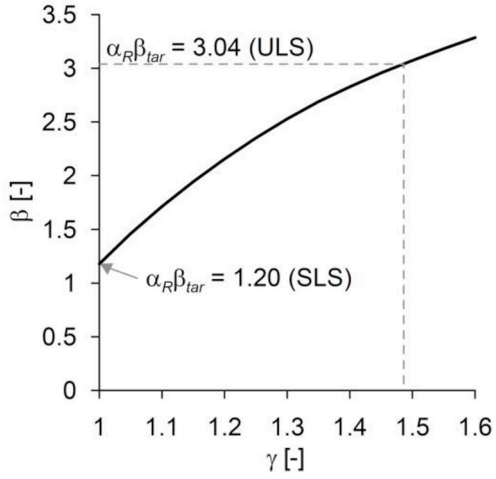

Fig. 16. Relationship between the partial factor in Eq. (16) and the reliability index.

A lower preload loss – or a lower partial factor – can be obtained in various ways. The following cases are studied:

- EN 1090 [3] assumes a coefficient of determination for the ratio between preload loss and applied torque of 0.06 (instead of the maximum allowed value of 0.1 in Refs. [35,36]). Using this coefficient of determination, whereas all other aspects remain as before, the required partial factor in ULS is: $\gamma = 1.45$.
- More relaxation tests applied for a longer period would allow for a reduction of the uncertainty. Assuming that M_C remains the same, but that S_C reduces to 0.10, the required partial factor in ULS is: $\gamma = 1.45$.
- The geometry studied has a width equal to the minimum value in Ref. [32], equal to $w = 2.4d_0$. The standard value in Ref. [32] is $w = 3d_0$. Using this value, the required partial factor in ULS is: $\gamma = 1.45$.
- The geometry studied has a relative summed thickness of $\sum T/d = 2.5$. If this value is increased to $\sum T/d = 5.0$, the required partial factor in ULS is: $\gamma = 1.40$.
- If all the above aspects are combined, the required partial factor in ULS is: $\gamma = 1.30$.

Annex D of EN 1090-3 [40] provides a procedure to determine the slip factor. This slip factor is similar to the friction coefficient, but it already implicitly accounts for short-term preload losses such as arising from lateral contraction, as it is derived from tests on loaded specimens. The prescribed specimens have a fixed and relatively large width of $w = 5d$, whereas we have demonstrated a significant dependency of the preload loss on the aluminium alloy and the geometry of the connection. This means that the slip factor cannot be directly applied to any aluminium connection; it must be adapted to account for alloy and geometry. Using the same procedure as described above, we derived a partial factor for the case that the slip factor is derived from this procedure and then used in a specimen of the same alloy and thickness, but with $w = 2.4d_0$ and also accounting for long-term preload losses, temperature variations, and uncertainty in the initial preload. That partial factor is $\gamma = 1.35$.

This study considered stainless steel bolts with an 0.2% proof stress that is at least 70% of the ultimate tensile strength. However [17] reports comparable preload loss in carbon steel as in stainless steel bolts. Similar results as reported here are therefore expected for aluminium plated slip resistant connections with preloaded carbon steel bolts. It is not surprising that the required reliability is not met in ULS with the default value of the partial factor ($\gamma = 1.25$), because this partial factor is equal to that in Ref. [41] prescribed for steel bolts in a steel plate assembly, whereas the preload loss in the latter configuration is lower for all causes studied in the previous chapter.

6. Conclusions

This paper presents a study into several causes of preload loss of high-strength stainless steel bolts (grade 316 – A4 80) in aluminium plated slip resistant connections. The following conclusions are drawn.

Significant preload loss results from viscoplastic behaviour, i.e. the combined effects of embedment creep, bolt relaxation, and aluminium plate creep. The combined effects provide an estimated preload loss between 6% and 20%, depending on the connection configuration. Retightening of bolts reduces embedment creep and aluminium creep can be reduced using cover plates of an alloy with an 0.2% proof stress that is not too low.

Another significant source of preload loss is related to lateral contraction of the plates due to an applied load. Combined with the stress in the plates caused by the preload, plasticity may occur in the plates in contact with the washers, especially in case these plates have a low 0.2% proof stress. Even if the 0.2% proof stress is high (e.g. 275 N/mm^2), lateral contraction may cause a preload loss of up to 8% for connections with widely applied geometry. This loss is significantly larger as compared to a steel plate assembly, mainly due to Young's modulus of aluminium being only one third of that of steel. Preload loss due to lateral contraction can be reduced by applying relatively thick cover plates.

A third source of preload loss is a temperature drop with respect to the assembly temperature. The preload loss is between 3% and 5% for a temperature drop of 30° Celsius.

Considering these preload loss sources together with the uncertainties of the initial preload and the friction coefficient, it appears that the current design model for slip resistance in EN 1999-1-1, does not meet the required reliability in the ultimate limit state, when applied to an aluminium plate assembly with high-strength stainless steel bolts. This type of connection can be used as a slip resistant connection, provided that 1) the partial safety factor for slip resistance is increased from 1.25 to 1.3–1.5 (depending on the connection configuration); and that 2) the bolts should be of a grade for which the 0.2% proof stress is at least 70% of its ultimate tensile strength.

Others have demonstrated that the viscoplastic behaviour of carbon steel high-strength friction grip bolts is of similar magnitude as for high-strength stainless steel bolts. Because the other sources of preload loss are independent of the type of bolt material, the same conclusion on partial factors is expected for aluminium plated slip resistant connections with carbon steel high-strength friction grip bolts.

The stiffness model in VDI combined with analytical, mechanics-based models allow for estimating the preload loss of any of the above causes, for a given connection configuration.

Author statement

Christiaan den Otter, was responsible for the experimental program and the prediction models for relaxation, creep, and temperature variations, He has reviewed the article text. Johan Maljaars, has developed the prediction model for lateral contraction and the framework for deriving partial factors, He has written the article text.

Declaration of competing interest

The authors declare that they have no known competing financial interests or personal relationships that could have appeared to influence the work reported in this paper.

Acknowledgements

The construction company Bayards is acknowledged for providing the specimens and the bolt load cells.

Appendix

The bolt stiffness k_b consists of a series spring system representing bolt head k_{SK}, the unthreaded shaft k_d, the threaded part located in the grip length k_t, and the threaded part in the nut k_{GM}. The plate assembly stiffness k_p consists of a series spring system representing washers k_w and plates $k_{\sum T}$, see Fig. 17. The springs representing the bolt and connection form the parallel system and the associated deformations are in equilibrium.where elastic stiffness of the subdivided parts are:

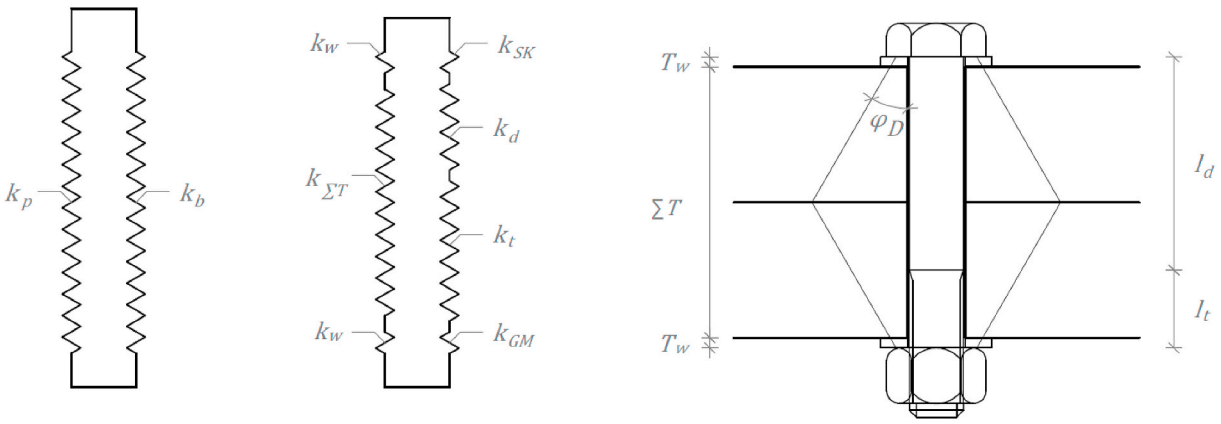

Fig. 17. Parallel spring model of VDI 2230 [11] containing bolt and connection with series spring stiffness (left) of a bolt and plate assembly (right).

The elastic bolt stiffness follows from:

$$k_b = \frac{1}{\frac{1}{k_{SK}} + \frac{1}{k_d} + \frac{1}{k_t} + \frac{1}{k_{GM}}} \tag{20}$$

$$\frac{1}{k_{SK}} = \frac{l_{SK}}{E_b A_d} = \frac{0.5d}{E_b A_d} \tag{21}$$

$$\frac{1}{k_d} = \frac{l_d}{E_b A_d} \tag{22}$$

$$\frac{1}{k_t} = \frac{l_t}{E_b A_t} \tag{23}$$

$$\frac{1}{k_{GM}} = \frac{1}{k_G} + \frac{1}{k_M} = \frac{l_G}{E_b A_{d_3}} + \frac{l_M}{E_b A_d} = \frac{0.5d}{E_b \frac{\pi}{4} d_3^2} + \frac{0.4d}{E_b A_d} \tag{24}$$

where:

A_d = nominal cross section unthreaded part
A_{d_3} = cross section of thread at minor diameter
d_3 = minor diameter of the bolt thread
l_{SK} = substitutional extension length for the deformation of the bolt head
l_d = length of the unthreaded part
l_t = length of the threaded part located in the grip
l_G = substitutional extension length for the deformation of the engaged thread
l_M = substitutional extension length for the deformation of the nut

The plate assembly stiffness follows from:

$$k_p = \frac{1}{\frac{1}{k_w} + \frac{1}{k_{\sum T}} + \frac{1}{k_w}} \tag{25}$$

A frustrum model is provided for the elastic stiffness of the different plate assembly parts, $k_{pp} \in (k_w, k_{\sum T})$:

$$k_{pp} = \frac{\pi E d_0 \tan \phi_D}{\ln\left(\frac{(2T \tan \phi_D + d_W - d_h)(d_W + d_h)}{(2T \tan \phi_D + d_W + d_h)(d_W - d_h)}\right)} \tag{26}$$

where d_W is the bearing surface outside diameter equal to $1.5d$ for the washers, or. $1.5d + T_w tan\phi_D$

References

[1] J. Shigley, Mechanical Engineering Design, McGraw-Hill, 1977.
[2] R. Bjorhovde, A. Colson, R. Zandonini, Connections in steel structures III, 1996, p. 438.
[3] EN 1090-2, Execution of Steel Structures and Aluminium Structures - Part 2: Technical Requirements for Steel Structures, CEN, Brussels, 2018, 2018.

[4] S. Duggal, Limit State Design of Steel Structures, Tata McGraw-Hill Education, 2014.
[5] K. Sai Ram, Design of Steel Structures, Pearson India, 2010.
[6] J. Berenbak, Evaluation tightening preloaded bolt assemblies according to EN 1090-2, 2012.
[7] EN 1993-1-4+A1:2015, Eurocode 3: Design of Steel Structures – Part 1-4: General Rules – Supplementary Rules for Stainless Steels, CEN, Brussels, 2015.
[8] N. Afzali, J. Pilhagen, T. Manninen, E. Schedin, N. Stranghöner, Preload losses in stainless steel bolting assemblies, Steel Constr. 10 (2017) 310–318.
[9] N. Stranghöner, D. Jungbluth, C. Abraham, A. Söderman, Tightening behaviour of preloaded stainless steel bolting assemblies, Steel Constr. 10 (2017) 319–332.
[10] N. Stranghöner, N. Afzali, P. De Vries, E. Schedin, J. Pilhagen, Slip factors for slip-resistant connections made of stainless steel, J. Constr. Steel Res. 152 (2019) 235–245.
[11] VDI 2230, Systematic calculation of high duty bolted joints, 2015.
[12] K.H. Brown, C.W. Morrow, S. Durbin, A. Baca, Guideline for Bolted Joint Design and Analysis, Sandia National Laboratories, Oak Ridge TN, 2008.
[13] J. Bickford, S. Nassar, Handbook of Bolts and Bolted Joints, Dekker inc., New York, 1998.
[14] T. Jaglinski, A. Nimityongskul, R. Schmitz, R.S. Lakes, Study of bolt load loss in bolted aluminum joints, J. Eng. Mater. Technol. 129 (2007) 48–54.
[15] E. Chesson, W.H. Munse, Studies on the behaviour of high-strength bolts and bolted joints University of Illinois. Engineering Experiment Station, Bulletin 469 (1965). http://hdl.handle.net/2142/4237.
[16] K. Shemwell, D.R. Johns, Long-Term Performance of Stainless Steel Fasteners - Final Report 7210-MA/819 EUR 1848 EN. European Commission, Technical Steel Research, 1997.
[17] N. Afzali, N. Stranghöner, J. Pilhagen, T. Manninen, E. Schedin, Viscoplastic deformation behaviour of preloaded stainless steel connections, J. Constr. Steel Res. 152 (2019) 225–234.
[18] P. Hradil, A. Chen, N. Baddoo, Numerical modelling of stainless steel preloaded bolted connections, Steel Constr. 10 (2017) 344–353.
[19] L.A. Deibler, Room Temperature Creep in Metals and Alloys, Sandia national laboratories, 2014.
[20] M. Rieth, A. Falkenstein, P. Graf, S. Heger, U. Jaentsch, M. Klimiankou, et al., Creep of the Austenitic Steel AISI 316 L(N) Experiments and Models (FZKA-7065), Institut fur Materialforschung., Germany, 2004.
[21] M.J. O'Brien, R.G. Metcalfe, High strength engineering Fasteners : design for fatigue resistance, J. Fail. Anal. Prev. 9 (2009) 171–181.
[22] ISO 68-1, ISO General Purpose Screw Threads — Basic Profile — Part 1: Metric Screw Threads, ISO, 1998, 1998.
[23] J.G. Kaufman, Properties of Aluminum Alloys, Aluminium Association & ASM international, Materials Park OH, 1999.
[24] J. Maljaars, F. Soetens, L. Katgerman, Constitutive model for aluminum alloys exposed to fire conditions, Metall. Mater. Trans. 39 (2008) 778–789.
[25] C. Kammer, Aluminium Taschenbuch – Grundlage und Werkstoffe, Beuth, 2009.
[26] C.F. Lucks, H.W. Deem, Thermal Properties of Thirteen Metals, ASTM International, West Conshohocken, PA, 1958, pp. 1–29, https://doi.org/10.1520/STP45025S.
[27] T.N. Chakherlou, M.J. Razavi, A.B. Aghdam, On the variation of clamping force in bolted double lap joints subjected to longitudinal loading: a numerical and experimental investigation, Strain 48 (2012) 21–29.
[28] W. Ramberg, W.R. Osgood, Description of Stress-Strain Curves by Three Parameters, Technical note 902, 1943. Naca.
[29] F.M. Mazzolani, Aluminium Alloy Structures, second ed., Spon, London, 1995.
[30] Abaqus Analysis User's Guide, Dassault Systèmes, 2014.
[31] J. Maljaars, D. Leonetti, C. Maas, Fatigue life prediction of hot riveted double covered butt joints, Int. J. Fatig. 129 (2019) 99–112.
[32] EN 1999-1-1+A1, Eurocode 9: Design of Aluminium Structures - Part 1-1: General Rules, CEN, Brussels, 2011, 2007.
[33] EN 1990+A1+A1/C2, Eurocode – Basis of Structural Design, CEN, Brussels, 2011, 2011.
[34] ISO 2394, General Principles on Reliability for Structures, fourth ed., 2015. ISO 2015.
[35] EN 14399-3, High-strength Structural Bolting Assemblies for Preloading – Part 3: System HG – Hexagon Bolt and Nut Assemblies, CEN, Brussels, 2015, 2015.
[36] EN 14399-4, High-strength Structural Bolting Assemblies for Preloading – Part 4: System HV – Hexagon Bolt and Nut Assemblies, CEN, Brussels, 2015, 2015.
[37] EN 14399-2, High-strength Structural Bolting Assemblies for Preloading – Part 2: Suitability Test for Preloading, CEN, Brussels, 2015, 2015.
[38] A.C.W.M. Vrouwenvelder, The JCSS probabilistic model code, Struct. Saf. 19 (1997) 245–251.
[39] JCSS Probabilistic Model Code. Part 3: Material Properties, JCCS, 2000. http://www.jcss.byg.dtu.dk/.
[40] EN 1090-3, Execution of Steel Structures and Aluminium Structures - Part 3: Technical Requirements for Aluminium Structures, CEN, Brussels, 2018, 2018.
[41] EN 1993-1-12006+C2+A1, Eurocode 3: Design of Steel Structures – Part 1-1: General Rules and Rules for Buildings, CEN, Brussels, 2014, 2014.